



ELSEVIER

Available online at www.sciencedirect.com

SCIENCE @ DIRECT®

Solar Energy Materials
& Solar Cells

Solar Energy Materials & Solar Cells 88 (2005) 199–208

www.elsevier.com/locate/solmat

Structural, optical and Raman scattering studies on DC magnetron sputtered titanium dioxide thin films

B. Karunagaran^a, Kyunghae Kim^a, D. Mangalaraj^{a,*},
Junsin Yi^a, S. Velumani^b

^a*School of Information and Communication Engineering, Sungkyunkwan University, Chunchun-dong, Jangan-gu, Suwon 440-476, Republic of Korea*

^b*Coordinación de Investigación y Desarrollo de Ductos, IMP, Eje Central Lázaro Cárdenas 152, D.F., C.P.07720, Mexico*

Received 1 September 2003; received in revised form 1 November 2003; accepted 1 March 2004

Available online 18 January 2005

Abstract

Thin films of TiO₂ were deposited by DC magnetron sputtering. The thicknesses of the films were measured using alpha step profilometer technique. Auger electron spectroscopy (AES) is used to determine the composition of the films. The influence of post-deposition annealing at 673 and 773 K on the structural, optical and Raman scattering was studied. The thicknesses of the films were found to be more or less the same irrespective of the annealing temperature and time. XRD results reveal the amorphous nature of the as-deposited film while the annealed samples were found to be crystalline with a tetragonal symmetry. Using the optical transmittance method, the optical constants such as band gap, refractive index and absorption coefficient were calculated and the influence of thermal annealing on these properties was reported. Raman study was employed to study the existence of different frequency modes and improvement of crystallinity of the TiO₂ films and the effect of annealing temperature on the Raman shift is studied and reported.

© 2004 Elsevier B.V. All rights reserved.

Keywords: TiO₂ thin films; Reactive sputtering; Optical constants; Raman scattering

*Corresponding author. Tel.: +82 312996570; fax: +82 312907159.

E-mail address: dmraj800@yahoo.com (D. Mangalaraj).

1. Introduction

Titanium dioxide is one of the extensively studied transition-metal oxides. The increased interest in both the application and the fundamental research of this material in the last decade stems from its remarkable optical and electronic properties. TiO₂ thin films have numerous applications due to their unique dielectric and optical properties. TiO₂ is a popular anti-reflective coating (ARC) in the photovoltaic (PV) industry due to its ease of deposition, low cost, and ideal optical properties. The use of TiO₂ thin films has many advantages, including their very good chemical resistance to the majority of chemicals used in the PV industry and their optimal refractive index for glass encapsulated silicon solar cells [1–3]. Generally, TiO₂ exists in three crystalline polymorphs: rutile (tetragonal), anatase (tetragonal) and brookite (orthorhombic). The anatase TiO₂ are found to exhibit interesting properties [4], which make it a promising material for gas sensors [5,6], solar cells [7,8] and dielectrics in semiconducting FETs [9]. These films present good durability and a high refractive index; hence they are suitable for applications such as multilayer optical coatings [10] and optical wave guides [11]. A large number of processing techniques such as sol–gel process [12], chemical vapor deposition [13], ion-assisted deposition [14] and sputtering [15] have been used to deposit TiO₂ thin films. The properties of the titanium oxide films depend not only on the preparation techniques but also on the deposition conditions. Even though many reports are available on the influence of annealing on the structural and optical properties of these films, the reports available for the effect of annealing and substrate temperature on the Raman scattering studies on TiO₂, especially TiO₂ in thin film form, are scarce. Hence an attempt has been made in this study to relate the effect of post-deposition annealing on the structural, optical and Raman scattering properties of titanium dioxide films prepared using the DC magnetron sputtering technique.

2. Experimental

Titanium oxide thin films were deposited onto well-cleaned p-type Si wafers (1 0 0) with a resistivity 8–10 Ω cm and also onto polished quartz substrates by using DC magnetron sputtering system. Pure titanium (99.999%) of 110 mm diameter and 2 mm thickness has been used as sputtering target. High-purity argon and oxygen were used as the sputtering and reactive gases, respectively. Rotary and diffusion pump combination was used to get the desired vacuum. The base pressure of the system is less than 10⁻⁵ mbar. After attaining the base pressure the oxygen partial pressure was set using a needle valve. Later on the argon was let in and sputtering pressure was maintained. In order to check the stability of the partial pressure, after each deposition argon flow was stopped and oxygen partial pressure was checked. It was confirmed to be at the set value. Such a practice is generally followed in reactive sputtering processes [16]. Before each run the target was pre-sputtered in Ar atmosphere for 5–10 min in order to remove the surface oxide layer of the target. All the depositions were carried out at a total pressure of 1 × 10⁻³ mbar. The distance

between the target and substrates was kept at 80 mm. The deposited film was annealed in air at temperatures 673 and 773 K for 1 h. The thicknesses of the as-deposited and annealed films were determined from step height measurements by an α -step stylus profilometer. The compositions of the films were analyzed using Auger electron spectroscopy (AES). The crystallinity was examined by using X-ray diffraction with $\text{CuK}\alpha$ radiation with steps of 0.02° with a fixed time scan and a time per step of 4 s. The transmittance of the films was measured in the visible region using a Jasco UV–VIS–NIR double beam spectrophotometer. Raman data were recorded using a Spex-1406 Ar-ion laser Raman spectrometer, Power 300 mW, and resolution 1 cm^{-1} .

3. Results and discussion

3.1. Thickness and composition

I – V characteristics of the titanium target were studied at different oxygen partial pressures while maintaining the working pressure at 1×10^{-3} mbar to determine the oxygen partial pressure at which the stoichiometric titanium dioxide films can be deposited. The details of the deposition condition are presented in our earlier work [17]. The surface roughness and thickness of the film was found to be 4.1 and 140 nm from α -step profilometer measurements. AES was performed on the sample surface to determine the Ti and O content in the film. The AES analysis was made at five different places of the sample and it was found that the composition was uniform throughout the sample with an O and Ti ratio 2.08.

3.2. Structural characterization

Fig. 1 shows the X-ray diffraction pattern of the as-deposited and annealed films. From the figure it was observed that the TiO_2 thin films deposited under ambient conditions are amorphous and the films annealed at higher temperatures are polycrystalline having tetragonal structure. The film annealed at 673 K shows both anatase [(1 0 1), (0 0 4)] and rutile (1 1 0) structure. But the films annealed at 773 K shows the predominant orientation with anatase phase with orientation along (0 0 4), (1 0 1) and (1 0 5) prominent reflections. The lattice parameters (a and c), grain size (D), dislocation density (δ) and microstrain, are calculated using the relevant formulas and correlated with the annealing temperature in Table 1. The calculated lattice constants ' a ' and ' c ' are found to agree well with the bulk ($a = 3.78$ and 9.52) values [18]. The grain sizes of the films are found to increase with the increase in annealing temperature. It was observed that the dislocation density (δ) and microstrain (ϵ) exhibit a decreasing trend with the annealing temperature, which leads to the reduction in the concentration of lattice imperfections [19].

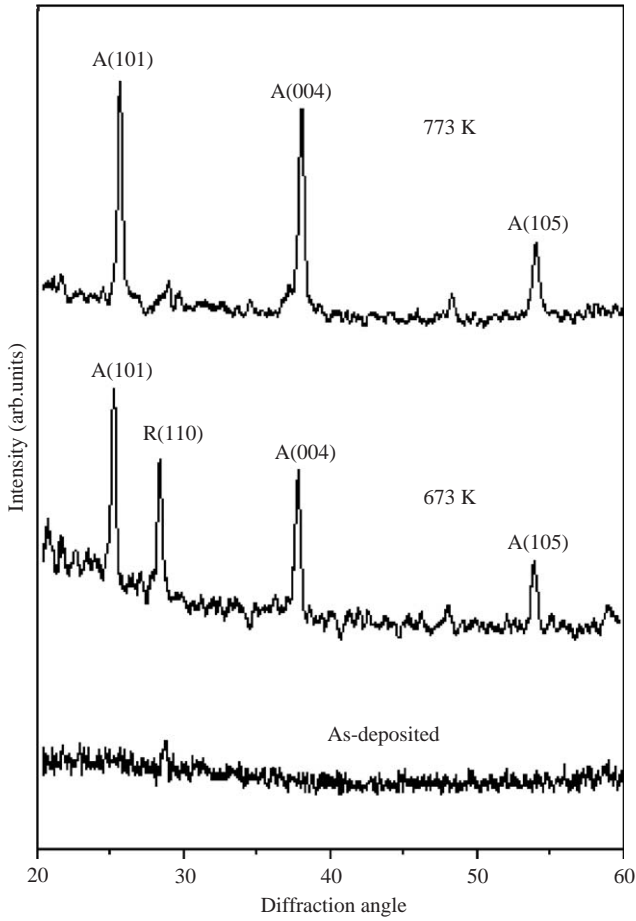


Fig. 1. X-ray diffraction pattern of an as-deposited and annealed (663 and 773 K) TiO_2 thin films.

Table 1
Structural parameters of annealed TiO_2 thin films

T_A (K)	2θ	$d(\text{Å})$	$[hkl]$	a (Å) calculated	c (Å) calculated	D (Å)	$\delta(10^{11}) \text{ cm}^{-2}$	$\varepsilon (10^{-3})$
673	25.14	3.5403	[1 0 1]	3.8130	9.5340	205	2.3795	1.4990
	37.72	2.3835	[0 0 4]					
	53.85	1.7015	[1 0 5]					
773	25.31	3.5169	[1 0 1]	3.7855	9.5048	235	1.8107	1.2913
	37.84	2.3762	[0 0 4]					
	53.97	1.6980	[1 0 5]					

3.3. Optical characterization

Fig. 2 shows the transmission spectrum of the annealed coatings (140 nm thick) in air for 1 h for different temperatures. It can be seen that the transmittance of the films decreases weakly when the materials are calcinated up to a temperature of 773 K. Since XRD analysis did not show a change of structure until 773 K, but only the presence of the anatase phase, it can be assumed that coatings becomes denser and denser with the annealing temperature. Then, the refractive index has been determined in order to show the densification. Fig. 3 illustrates the evolution of refractive indexes as a function of wavelength for titanium oxide films annealed in air at 673 and 773 K and as-deposited. It can be seen that the refractive indexes of the films increases with the annealing temperature. The variation of absorption coefficient and extinction coefficient with the annealing temperature are depicted in Figs. 4 and 5, respectively. It is seen that the main tendency of both these optical coefficients is to increase with the increase of calcinations. So, the evolution of the extinction coefficient can be related to the variation of transmittance. The decrease in transmittance results in the increase of the extinction coefficient. It can be supposed that the compactness of titanium oxide films changes from a porous structure to a dense structure. This means that the packing density of the films increases with the increase of annealing temperature.

Since TiO_2 is a semiconductor with a large band gap [20–22], the optical band gap E_g can be determined from absorption coefficient α . The sharp decrease in the transparency of the films in the UV region is caused by the fundamental light absorption in the semiconductor. The absorption coefficient α , which depends on the wavelength λ , can be obtained by using the following relation. When scattering

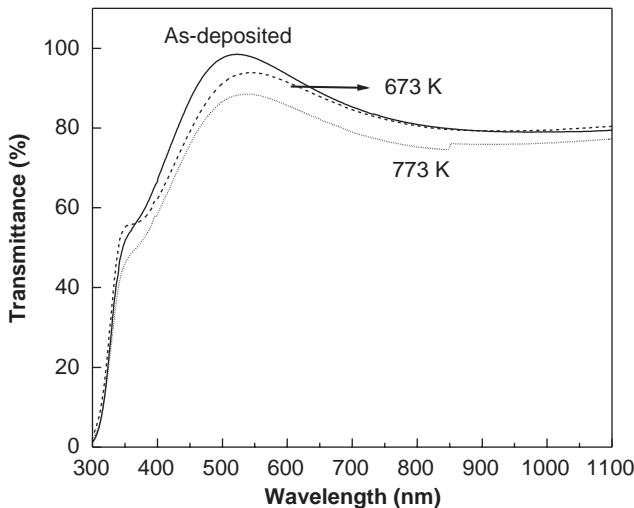


Fig. 2. Variation of transmittance with the wavelength for an as-deposited and annealed (663 and 773 K) TiO_2 thin films.

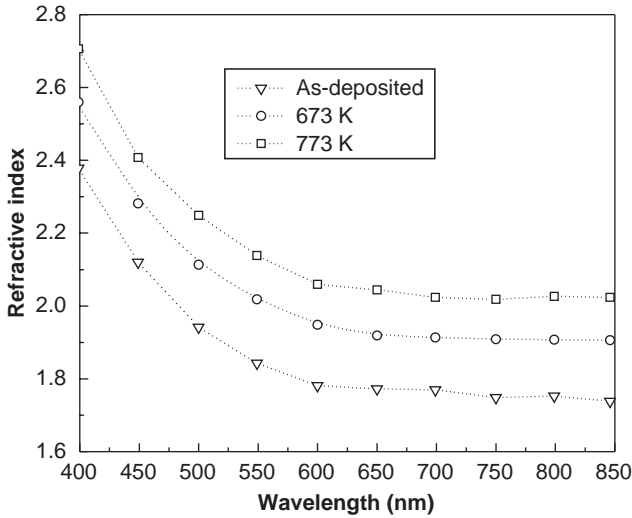


Fig. 3. Plot of refractive index against the wavelength of as-deposited and annealed TiO₂ thin films.

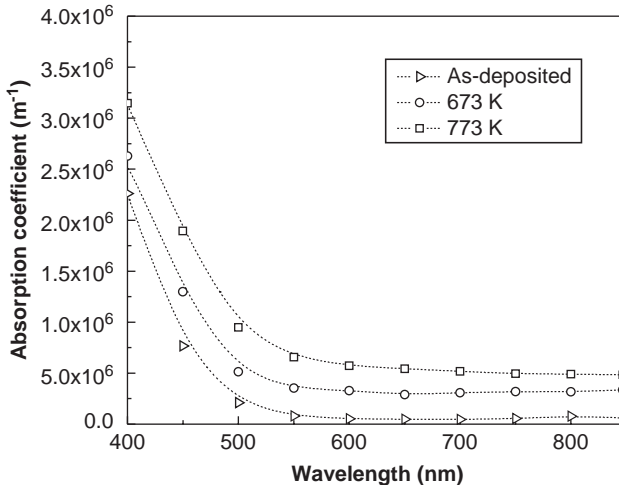


Fig. 4. Change of absorption coefficient with wavelength of as-deposited and annealed TiO₂ thin films.

effects are neglected, the absorption coefficient may be expressed by

$$\alpha \propto (h\omega - E_g)^m,$$

where E_g is the optical band gap. For the indirect allowed transitions, $m = 2$, but for the direct forbidden transitions, $m = 1.5$ [23]. Both experimental results and theoretical calculations suggest that TiO₂ has a direct forbidden gap (3.03 eV), which is almost generated with an indirect allowed transition [20,23]. Due to the

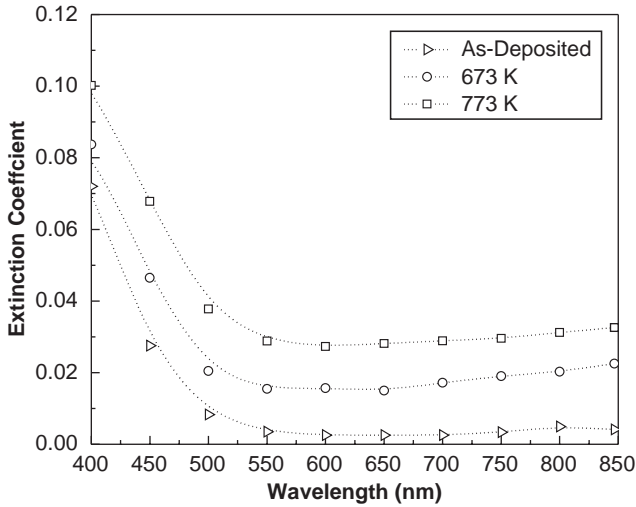


Fig. 5. Variation of extinction coefficient with the wavelength for an as-deposited and annealed (663 and 773 K) TiO₂ thin films.

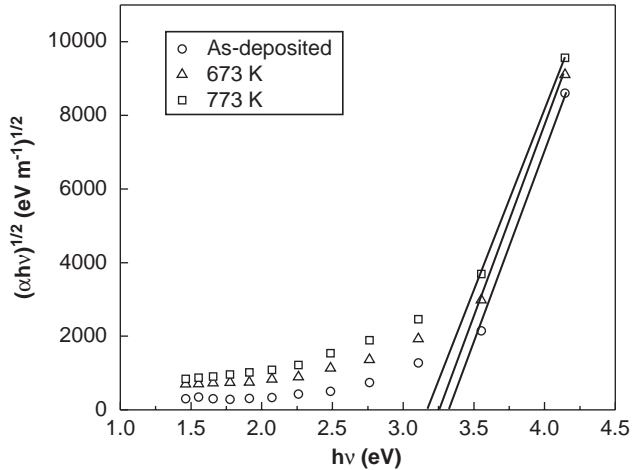


Fig. 6. $(\alpha hv)^{1/2}$ vs. $h\nu$ plots of the TiO₂ films at different annealing conditions.

weak strength of the direct forbidden transition, the indirect allowed transition dominates in the optical absorption just above the absorption edge [23]. Then the absorption coefficient above the threshold of the fundamental absorption follows the $(E - E_g)^2$ energy dependence characteristic of indirect allowed transitions as illustrated by the $\alpha^{1/2}$ vs. photon energy (E) plot. The $(\alpha hv)^{1/2}$ vs. $h\nu$ plots for the TiO₂ films at different annealing conditions are shown in the Fig. 6. The indirect band gaps of the films of different thickness are evaluated from the x-axis intercepts

of the plot. The extrapolated optical absorption gaps of films have been determined. It can be seen that the optical band gap decreases (3.32 to 3.17 eV) when the annealing temperature increases. Radecka et al. [24] obtained similar evolution of E_g with the temperature. Then, it can be supposed that the variation of density and the structural modifications may be responsible for changes in the shape of the fundamental absorption edge.

3.4. Raman scattering studies

The anatase form of titanium dioxide is tetragonal with space group D_{4h}^{19} [25]. Earlier, factor group analysis indicates the existence of 15 optical modes in the anatase TiO_2 with the irreducible representations, $1A_{1g} + 1A_{2u} + 1B_{1g} + 1B_{2u} + 3E_g + 2E_u$. Among these modes A_{1g} , B_{1g} and E_g are Raman active and those of A_{2u} , B_{2u} and E_u are infrared active [26].

Films of thicknesses 140 nm are calcinated in air in a Muffle oven for 1 h at 673 and 773 K. After each calcination, the Raman spectrum was recorded. The results are shown in Fig. 7 along with the Raman spectra of the pure p-type silicon as an inset in the film. In order to project the existence of different modes clearly in the calcinated film spectra, the Raman shift ranges from 514 to 580 where no feature of TiO_2 was observed and were deleted from the spectrum. The frequencies of the Raman bands are identified using a Gaussian peak fit software and they were 637, 513, 396, 195.1 and 144.3 cm^{-1} , which agree well with those in previous studies for anatase powder and single crystals [27,28]. Based on the factor group analysis the 396 cm^{-1} peak is assigned to the B_{1g} mode (ν_4), 637 cm^{-1} peak can be attributed to the E_g mode (ν_1),

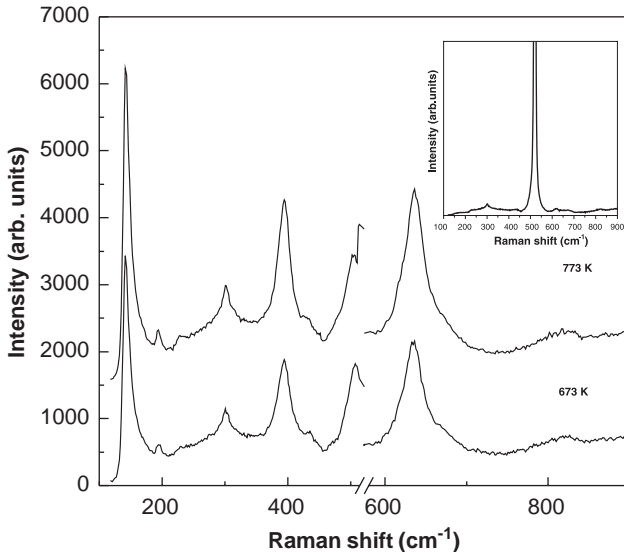


Fig. 7. Raman spectra of the TiO_2 thin films of thickness 140 nm annealed at 673 and 773 K (Inset—Raman spectra of a p-type Si substrate).

Table 2
Observed Raman shift (cm^{-1}) and their assignment of TiO_2 film

Present work	Seikiya et al. [27]	Ohsaka et al. [28]	Xu et al. [29]	Assignments
ν_1 637	638.6	639	636	E_g
ν_2 513	515.3	519	512	B_{1g}
ν_3 513	515.2	513	512	A_{1g}
ν_4 396	396.6	399	396	B_{1g}
ν_5 195.1	197.2	197	192	E_g
ν_6 144.3	144.5	144	145	E_g

513 cm^{-1} peak can be attributed to the $A_{1g} + B_{1g}$ modes ($\nu_2 + \nu_3$) [29]. From the factor plane analysis it was observed that the A_{1g} (ν_3) and B_{1g} (ν_2) both involve the Ti–O bond stretching normally to the film plane. The peaks at 195.1 and 144.3 cm^{-1} are assigned to the E_g modes represented by ν_5 and ν_6 . The Raman shift observed in the present study along with their assignment and comparisons with the other reports are presented in Table 2.

In the case of the annealed films, there is no significant change in the peak position but the intensity of the peaks increase with the increase in the annealing temperature. The peak position, FWHM, intensity and area under the peak are calculated using a Gaussian peak fit software. The FWHM corresponding to the peak at 396 cm^{-1} is found to be 29.08 and 23.03 for films annealed at temperatures 673 and 773 K, respectively, indicating a decrease in FWHM from 29.08 to 23.03 on annealing and the FWHM in all the other peaks are also found to decrease with the increase in the annealing temperature. The increase of intensity of the peaks, the area under the curve and the decrease of FWHM can be attributed to the improvement in the crystallinity of the annealed films, which was clearly seen from the well-defined XRD peaks of the annealed samples.

4. Conclusion

Titanium dioxide thin films have been deposited by DC magnetron sputtering and the films were annealed at different temperatures in air. The AES analysis has shown that the films deposited are stoichiometric. XRD and Raman spectroscopy both show that the as-deposited TiO_2 films are basically amorphous but their structure is converted to the anatase crystalline phase when the films are annealed at higher temperatures which is supported by the increase of refractive index (evaluated from optical transmittance). UV–VIS spectroscopy showed that as-deposited and annealed films are highly transparent, it was also found that the band gap of the films decrease with the increase of annealing temperature.

Acknowledgement

One of the authors (S.V.) acknowledges the financial support received through the project CONACYT G38618-U.

References

- [1] B.S. Richards, J.E. Cotter, C.B. Honsberg, S.R. Wenham, Proceedings of 28th IEEE Photovoltaic Specialists Conference, 2000, p. 375.
- [2] B.S. Richards, J.E. Cotter, C.B. Honsberg, *Appl. Phys. Lett.* 80 (2002) 1123.
- [3] B.S. Richards, S.F. Rowlands, A. Ueranatasun, J.E. Cotter, C.B. Honsberg, *Sol. Energy* 76 (2004) 269.
- [4] T. Tang, K. Prasad, R. Sanjines, P.E. Schmid, F. Levy, *J. Appl. Phys.* 75 (1994) 2042.
- [5] M. Ferrara, *Nanostruct. Mater.* 7 (1996) 709.
- [6] H. Tang, *Sensor. Actuat. B Chem.* 26 (1995) 71.
- [7] K.S. Yeung, Y.W. Lamb, *Thin Solid Films.* 109 (1993) 242.
- [8] M.K. Nazeeruddin, *J. Amer. Chem. Soc.* 115 (14) (1993) 6387.
- [9] D.C. Gilmer, *Chem. Vapour Depos.* 4 (1998) 9.
- [10] Y. Sawada, Y. Taga, *Thin Solid Films* 116 (1984) 155.
- [11] K.L. Siefering, G.L. Griffin, *J. Electrochem. Soc.* 137 (1990) 1206.
- [12] Jimmy C. Yu, Jiaguo Yu, Jincai Zhao, *Appl. Catal. B: Environ.* 36 (2002) 31.
- [13] J.P. Lu, J. Wang, R. Raj, *Thin Solid Films* 204 (1991) L13.
- [14] S. Miyaki, T. Kobayashi, M. Satou, F. Fijimoto, *J. Vac. Sci. Technol. A* 9 (1991) 3036.
- [15] D. Mardare, P. Hones, *Mater. Sci. Eng. B* 68 (1999) 42.
- [16] M.H. Suhail, G. Mohan Rao, S. Mohan, *J. Appl. Phys.* 71 (1992) 1421.
- [17] B. Karunagaran, R.T. Rajendra Kumar, D. Mangalaraj, Sa.K. Narayandass, G. Mohan Rao, *Crys. Res. Technol.* 37 (12) (2002) 1285.
- [18] *Natl. Bur. Stand. (U.S) Monogr.* 1969, 25, 82. JCPDS database no. 21-1272.
- [19] P.K.R. Kalita, B.K. Sharma, H.L. Das, *Bull. Mater. Sci.* 23 (2000) 313.
- [20] K.M. Glassford, J.R. Chelikowsky, *Phys. Rev. B* 46 (1992) 1284.
- [21] T. Fujii, N. Sakata, J. Takada, Y. Miura, Y. Daitoh, M. Takano, *J. Mater. Res.* 9 (1994) 1468.
- [22] H. Tang, H. Berger, P.E. Schmid, F. Levy, *Solid State Commun* 92 (1994) 267.
- [23] N. Daude, C. Gout, C. Jounain, *Phys. Rev. B.* 15 (1977) 3229.
- [24] M. Radecka, K.Z. Akrczewska, H. Czternastek, T. Stapinski, S. Debrus, *Appl. Surf. Sci.* 65/66 (1993) 227.
- [25] M. Horn, C.F. Schwerdfeger, E.P. Meagher, *Z. Kristallogr.* 136 (1972) 274.
- [26] T. Seikiya, S. Ohta, S. Kamei, M. Hanakawa, S. Kurita, *J. Phys. Chem. Solids* 62 (2001) 717.
- [27] I.R. Beattie, T.R. Gilson, *Proc. R. Soc. London, Ser. A* 307 (1967) 407.
- [28] T. Ohsaka, F. Izumi, Y. Fujiki, *J. Raman Spectrosc.* 7 (1978) 321.
- [29] Wei-Xing Xu, Shu Zhu, Xian-Cai Fu, Qiang Chen, *Appl. Surf. Sci.* 148 (1999) 253.